Observing long-term changes in rice phenology using NOAA–AVHRR and DMSP–SSM/I satellite sensor measurements in Punjab, India

R. P. Singh*, S. R. Oza and M. R. Pandya

Agro-Ecology and Management Division (ARG/RESIPA), Space Applications Centre (Indian Space Research Organization), Ahmedabad 380 015, India

The paper reports a unique observation from remote sensing records that the temporal rice growth pattern in terms of time of emergence and peak vegetation stage has been advanced by 3–4 weeks in Punjab, India from 1981 to 2000. Analysis was carried out using multi-temporal remote sensing data from the optical sensors such as Advanced High Resolution Radiometer (AVHRR) and the passive microwave sensors such as Special Sensor Microwave Imager (SSM/I) onboard NOAA and DMSP series of satellites respectively. The rice growth characteristics were quantified by Badhwar and Gaussian model fitting on seasonal Normalized Difference Vegetation Index (NDVI) covering the monsoon period (kharif season) for six years. The observed time of peak vegetation stage of rice estimated from the average growth profile of years 1981–82 was 4 September, which advanced to 8 August in years 1999–2000. This change in phenology was further confirmed using Basist Wetness Index (BWI) data derived using multi frequency approach. The BWI data representing surface moisture/water fraction were found to reach maximum in the middle of July in 1988, compared to middle of June in 1998. Temporal trends in mean BWI of Punjab during May–June also indicate a shift in crop growth profile and gradual increase in area flooded with water for rice transplanting with time.

Keywords: Crop, phenology, remote sensing, microwave.

QUANTIFICATION of human-induced land use/cover changes and their impact on regional climate is an important area of global change research[1,2]. It has been demonstrated that large-scale changes in crop irrigation and deforestation appreciably affect climate[3–5]. Remote sensing-based studies have been used to highlight the effect of changing vegetation phenology[6], global net primary productivity[7] and global land use/cover on climate. Indian agriculture has undergone significant change for the past several decades. Pandya *et al.*[8] have reported increase in vegetation activity over the years in India using NOAA–AVHRR-derived fraction of absorbed photosynthetically active radiation data. Amongst the major changes in Indian agriculture has been the introduction of irrigated rice in the semi arid northwest Indian region. Punjab has witnessed significant change in cropping pattern during the last few decades[9]. Increase in rice area is of particular significance. Rice–wheat rotation followed in Punjab leaves little time for land preparation for wheat after rice. This has resulted in a shift of the rice calendar. The cropping pattern shifts are generally described in terms of crop dominance only, while equally important changes in phenology are much less studied, as they are not captured in crop statistics information. Multi-temporal remote sensing data are well suited to study crop phenology. Satellite remote sensing in optical wavelengths is sensitive to changes in photosynthesis and biomass, while microwave remote sensing can detect surface soil-moisture conditions. In this study we have investigated the synergistic use of coarse resolution optical and microwave data in detection of (a) shift in rice crop phenology using six-year Normalized Difference Vegetation Index (NDVI) temporal profile from the period 1981 to 2000 and (b) changes in flooded-field condition associated with rice crop using seven year Basist Wetness Index (BWI)[10] data from the period spanning 1988 to 2000.

The State of Punjab, with a geographical area of 50, 362 km^2, occupies a special place in Indian agriculture. It contributes around 70% of wheat and 50% of rice in the national pool of foodgrains. It lies between 29°33′–32°31′N lat. and 73°53′–76°55′E long. The climate is dominantly sub-tropical, semi-arid and monsoon-type. Most of the soils of Punjab, which are part of the Indus plains are derived from alluvium, and are deep. The soil texture varies from sandy to fine silty, with majority belonging to coarse loamy (62.3%) and fine loamy (19.5%). Punjab is a vast expanse of flat alluvial land, except Shiwalik hills in the North; fluvial carvings and deposits of the three major rivers (Ravi, Beas and Sutluj) in the central Punjab and sand dunes in the southwest[9].

Crops show a characteristic temporal spectral behaviour due to growth and senescence[11]. It has been observed in a number of investigations[12,13] that the profile of spectral development of a crop, as monitored through a vegetation index derived from remotely sensed data, offers unique advantage in growth stage and yield estimation. The time of crop emergence and senescence is of particular importance because of their considerable influence on the spatial and inter-annual variability of terrestrial carbon cycles. Large-scale carbon cycling models requires a regional-scale phenology model to capture mean phenological changes related to average environmental conditions for each grid. NDVI data derived from NOAA–AVHRR sensor under Pathfinder project were used to model the rice growth profile over homogenous rice-dominated agricultural grid (0.5° × 0.5°), covering parts of Punjab (75.5–76°E and 30.5–31°N). Ten-day maximum value composite NDVI data of kharif season (from first week of June to November) were analysed for six years, viz. 1981, 1982,

*For correspondence. (e-mail: rpsingh@sac.isro.gov.in)

1996, 1997 and 1999 and 2000. NDVI data used in the analysis were provided by Goddard Space Flight Center, Distributed Active Archive Center, USA.

Originally, the concept of NDVI was developed to exploit the spectral properties of leaves of green plants, which absorb incoming radiation in red wavelength of the optical spectrum (AVHRR red channel: 0.62–0.70 μm) and strongly reflect light in the near-infrared wavelength (AVHRR NIR channel: 0.74–1.1 μm). NDVI is derived using the red reflectance (ρ_r) and near-infrared reflectance (ρ_n) as:

$$\text{NDVI} = \frac{(\rho_n - \rho_r)}{(\rho_n + \rho_r)} \text{ (when } \rho_n > 0 \text{ and/or } \rho_r > 0), \quad (1)$$

$$\text{NDVI} = 0 \quad \text{(when } \rho_n, \rho_r = 0).$$

The reflectance of vegetation in red (ρ_r) is governed by the chlorophyll absorption and the reflectance in near-infrared (ρ_n) is due to the phenomenon of total internal reflectance occurring within the leaf. There is decrease in ρ_r and increase in ρ_n and NDVI as the crop grows. NDVI has low values ranging from –0.2 to 0.1 for snow and bare soil, glaciers, rocks, and rises to around 0.2 to 0.8 for green vegetation. NDVI is an estimator of fraction of absorbed photosynthetically active radiation used by leaves in photosynthesis. NDVI is frequently used by various researchers in modelling biospheric processes and climate. Earlier studies using long term NDVI data have revealed large-scale inter-annual variations in global vegetation activity related to climate[14]. NDVI anomalies in semi-arid tropics have been reported to correlate well with equatorial Pacific sea surface temperature anomalies associated with El Nino southern oscillation phenomenon[15]. NDVI datasets have also indicated a warming-driven greening trend consistent with the observation of increased amplitude of the seasonal cycle of atmospheric CO_2 data from the North[16,17].

Various NDVI datasets are available with different spatial and temporal resolutions with different temporal periods. The NOAA–AVHRR sensors cover long-term time series NDVI datasets from 1981 to the present. Other NDVI data are also available from Landsat-Thematic Mapper (1984 to 2003), EOS-MODIS (2000 to the present) and SPOT–VEGETATION data (1998 to the present). Pettorelli *et al.*[18] have reviewed in detail different satellite-derived NDVI datasets and their environmental applications. The NOAA–Pathfinder AVHRR Land (PAL) NDVI data product at 8 km resolution is a well-calibrated dataset for long-term studies[19]. The pathfinder NDVI dataset is corrected for Rayleigh scattering and ozone absorption using radiative transfer model by Gordon *et al.*[20]. Inter sensor calibrations have been accounted by fitting a time-dependent calibration algorithm[21] for each channel to normalize the instrumental degradation of each satellite of the NOAA series flown from period 1981.

To analyse the crop growth parameters, viz. time of emergence and peak period, temporal modelling of the NDVI data was carried out by two approaches. In the first approach, a nonlinear growth function was fitted as described by Badhwar[11]:

$$\text{NDVI}(t) = \text{NDVI}_0 (t/t_0)^{\alpha} \exp(-\beta(t^2 - t_0^2)) \text{ for } t > t_0, \quad (2)$$
$$= \text{NDVI}_o \text{ for } t \le t_0.$$

where NDVI (t) represents the crop greenness at time t, NDVI_0 is the soil NDVI at the spectral emergence day (t_0), and α, β are crop-specific constants ($\alpha > 0$ and $\beta > 0$). In the second approach, the temporal growth pattern was fitted using Gaussian function:

$$\text{NDVI}(t) = \text{NDVI}_m \exp(-(t - t_m)^2/2\sigma^2), \quad (3)$$

where NDVI_m is NDVI at peak vegetative stage (t_m) and σ represents the width of the profile. The above model fittings were carried out after the scaled NOAA-AVHRR NDVI (in Digital Number (DN)) were converted to crop NDVI as:

$$\text{NDVI} = (\text{NDVI}_{DN} - 128.0)*0.008. \quad (4)$$

Optical remote sensing data are not sensitive in detecting the low NDVI at the time of crop emergence, at the same time passive microwave radiometers show enhanced sensitivity in detection of surface water fraction available at the time of field preparation during rice transplanting. We have used SSM/I sensor data flown on-board a series of Defense Meteorological Satellite Program (DMSP) platform, to study changes in surface wetness conditions. SSM/I is a seven-channel passive microwave radiometer operating at four frequencies (19.35, 22.235, 37.0 and 85.5 GHz) and dual-polarization (except at 22.235 GHz which is V-polarization only). Multiple frequencies available[22,23] on the SSM/I instrument have different responses to the liquid water on land, and this response across the microwave spectrum indicates the percentage of the 'radiating surface' that is water. Wang and Schmugge[24] developed a model for computing the emissivity of wet surface based on the dielectric constant of water. As the fractional amount of wet surface increases, its emissivity decreases. The lowest emissivity occurs when the surface becomes saturated with water, as in the case of flooded land. The reduction in soil emissivity (from dry to wet condition) is large when observed in low frequencies (19.35 GHz) compared to high frequencies (85.5 GHz). The relative change in emissivity between two or more frequencies is approximated as:

$$\Delta\varepsilon = \beta_0 [\varepsilon(f_2) - \varepsilon(f_1)] + \beta_1 [\varepsilon(f_3) - \varepsilon(f_2)], \quad (5)$$

where f_1, f_2, and f_3 represent the 19, 37 and 85 GHz vertical channels respectively, and β_0, β_1 are proportionality constants. To quantify the surface wetness condition, Basist *et al.*[10] have defined BWI as:

Table 1. Growth profile of rice using NOAA Pathfinder AVHRR Land NDVI data based on Badhwar model. Time (t) is considered from 1 May for fitting profile parameters

Year	$NDVI_0$	t_0	Alpha	Beta (10^{-4})	t_m	r	N	SEE
1981–82	0.02891	48.4825	5.4321	1.6778	127.26	0.9728	14	0.0422
1996–97	0.06565	35.6168	3.2866	1.3913	108.58	0.9880	14	0.0284
1999–00	0.01514	25.0482	3.9636	1.9733	100.22	0.9798	14	0.0416

Table 2. Growth profile of rice using NOAA Pathfinder AVHRR Land NDVI data based on Gaussian model. Time (t) is considered from 1 May for fitting profile parameters

Year	$NDVI_m$	t_m	σ	r	N	SEE
1981–82	0.5331	128.64	37.47	0.982	14	0.0326
1996–97	0.5938	112.16	41.70	0.985	14	0.0304
1999–00	0.5738	103.22	35.71	0.978	14	0.0416

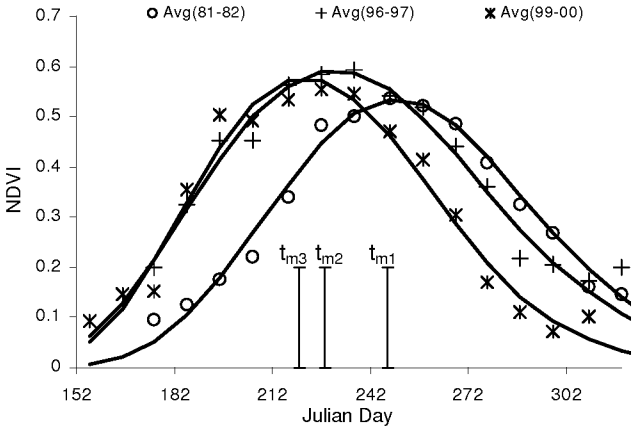

Figure 1. Average NDVI growth profile of rice-dominated grid estimated using NOAA–AVHRR NDVI data during kharif season and model fit over 0.50 grid covering Ludhiana district, Punjab. t_{m1}, t_{m2}, t_{m3} represents mean peak vegetative stage of crop during 1981–82, 1996–97 and 1999–2000 respectively.

$$BWI = \Delta\varepsilon T, \tag{6}$$

where T is the surface temperature. The weekly composite BWI data from National Climatic Data Centre (NOAA/NESDIS) at 0.3° resolution were used in assessment of surface flooding. The weekly composting scheme is used to generate global gridded product from swath data at regular temporal period and to avoid the atmospheric influence in assessment of land surface wetness condition. The average surface wetness for the whole of Punjab for three pre-monsoon weeks, viz. (1) 14–20 May, (2) 28 May–3 June and 4–10 June was analysed for seven years (1988, 1992, 1995, 1997, 1998, 2000 and 2002). The temporal weekly profiles of surface wetness for Punjab during kharif season were analysed (April–August) for two representative years, viz. 1988 and 1998 separated by a decade.

The estimated model parameters of crop growth for Badhwar and Guassian model are given in Tables 1 and 2 respectively. The observed mean and fitted profile for Badhwar is shown in Figure 1. The temporal NDVI patterns capture crop emergence, greening, peak vegetative phase and senescence. The NDVI composite over a ten-day period is affected by continuous clouds, varying solar and view zenith angles and other sources of variability such as vegetation anisotropy, etc. Since our objective was to infer long-term changes in rice phenology and avoid other error sources, the average NDVI profile for consecutive years, i.e. 1981–1982, 1996–1997 and 1999–2000 were analysed. The derived dates for the peak growth stages using Badhwar model were 4 September during 1981–82, 16 August during 1996–97 and 8 August in 1999–2000. Thus, there was a shift of 27 days in the occurrence of peak crop growth stage (t_m) from 1981–82 to 1999–2000 season. The dates derived using Gaussian model closely match those of the Badhwar model. This indicates that the type of model used to characterize crop growth behaviour does not significantly affect the result. Since the above profile was generated for a site belonging to the traditional rice-growing area, north of Ludhiana, Punjab, it can be assumed that the phenology represents the rice crop for all the years.

The wetness index was used to further confirm the above estimated shift in growth cycle. Since the transplanting of rice crop is associated with field-flooding, the BWI representing surface moisture changed significantly. The results of temporal trends in mean wetness computed for weekly composite sets with median dates at 17 May, 31 May and 7 June respectively, are shown in Figure 2. We have analysed the weekly wetness trends for the seven years spanning 1988 to 2002 to find out the earliest week, which is most affected due to shifting rice growth characteristic. The mean wetness index observed on 17 May was found almost constant over the years (slope = 0.13, r = 0.53). Increasing trend was found on 31 May (slope = 0.82, r = 0.88) and 7 June (slope = 0.99, r = 0.86). It can be inferred from the scatter in the time trend of surface wetness in Figure 2, that field preparation/puddling activities are now being initiated during the last week of May. Relative increase in the amount of wetness during these weeks over the years from 1988 indicated increase in area under flooding. It should be mentioned that the rice area in Punjab has increased from 1.18 Mha during 1981 to 2.61 Mha in 2001.

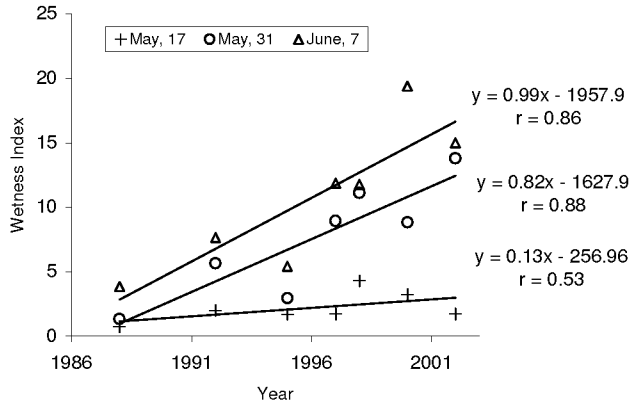

Figure 2. Inter-annual variability of mean surface wetness in pre-monsoon period from 1988 to 2002 in Punjab using SSM/I data.

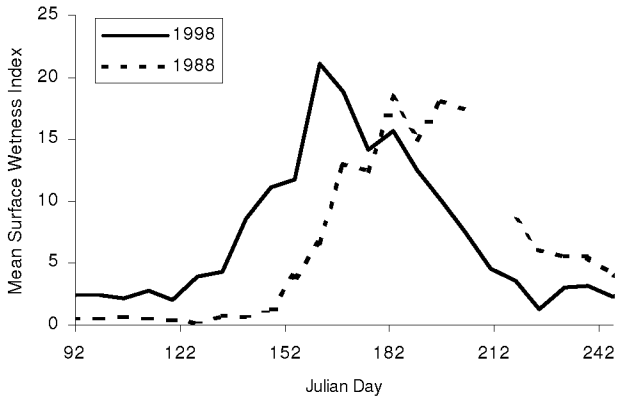

Figure 3. Seasonal variations of mean surface wetness of Punjab during kharif season for two representative years (1988, 1998).

The decadal change in temporal pattern of surface wetness was analysed to study the peak wetness period. Figure 3 shows the mean surface wetness temporal profile of 1988 and 1998 of the whole study region. Peak wetness in 1998 was observed in the middle of June compared to middle of July in 1988. Evidence of irrigation activities in May can be observed in the 1998 wetness profile compared to irrigation in June in the 1988 wetness profile (Figure 3). Thus, a four-week early shift in puddling/transplanting activity from 1988 to 1998 can be concluded. This observation matches well with similar shift observed in peak growth stage derived from NDVI data.

This investigation shows the utility of space borne AVHRR and SSM/I data for studying the long-term changes in agriculture. The growth profile study using temporal NDVI and wetness index data reflected well the changes in the agricultural scenario of Punjab over the last two decades. The peak growth stage derived using NDVI data and the pudlling/transplanting period derived from SSM/I wetness index showed an earlier 3–4 weeks shift in rice planting dates over the years in Punjab. Surface wetness also showed that a large fraction of agricultural area is becoming wetter over the years, coinciding with the increase in rice cultivation. High temporal data like AVHRR, irrespective of the coarse spatial resolution, could capture the dynamics of agricultural activities due to their high temporal resolution. SSM/I data though not designed for land surface studies have been found useful due to their inherent characteristic signature for regional soil moisture studies and flooding condition assessment[25–27]. This study shows the potential of detecting the rice planting period mainly due to the puddling operation that changes the surface wetness significantly. This was mainly due to the large monoculture cultivation pattern of rice crop in Punjab. The potential of this sensor can be best utilized for agricultural study with an improved spatial resolution. There exist strong and convincing evidence that modification of land-cover properties affects partitioning of available energy and water, which can influence local to regional-scale climate. The large-scale modifications in land-cover properties such as increase in wetness and advancement in the onset of vegetation greening in summer would result in extra evaporation and changes in atmospheric CO_2 seasonality. A modelling study using appropriate land-surface model coupled with remote sensing-derived crop phenology and soil moisture is needed to quantify the integrated influence of increase in rice crop area and changes in phenology on regional climate.

1. Wang, H., Pitman, A. J., Zhao, M. and Leemans, R., The impact of land cover modification on the June meteorology of China since 1700, simulated using a regional climate model. *Int. J. Climatol.*, 2003, **23**, 511–527.
2. Zhao, M., Pitman, A. J. and Chase, T., The impact of land cover change on the atmospheric circulation. *Climate Dyn.*, 2001, **17**, 467–477.
3. Bonan, G. B., Pollard, D. and Thompson, S. L., Effect of boreal forest vegetation on global climate. *Nature*, 1992, **359**, 716–718.
4. Shukla, J. and Mintz, Y., Influence of land surface evapotranspiration on the earth's climate. *Science*, 1982, **215**, 1498–1500.
5. Nemani, R. R., Running, S. W., Pielke, R. A. and Chase, T. N., Global vegetation cover change from coarse resolution satellite data. *J. Geophys. Res. D*, 1996, **101**, 7157–7162.
6. Myneni, R. B., Keeling, C. D., Tucker. C. J., Asrar, G. and Nemani, R. R., Increased plant growth in the northern high latitudes from 1981–1991. *Nature*, 1997, **386**, 698–702.
7. Nemani, R. R. *et al.*, Climate driven increase in global terrestrial net primary production from 1982 to 1999. *Science*, 2003, **300**, 1560–1563.
8. Pandya, M. R., Singh, R. P. and Dadhwal, V. K., A signal of increased vegetation activity in India from 1981 to 2001 observed using satellite-derived fraction of absorbed PAR. *Curr. Sci.*, 2004, **87**, 1122–1126.
9. Ray, S. S., Sood, A., Das, G., Panigrahy, S., Sharma, P. K. and Parihar, J. S., Use of GIS remote sensing for crop diversification – A case study for Punjab State. *J. Indian Soc. Remote Sensing*, 2005, **33**, 181–188.
10. Basist, A., Grody, N., Peterson, T. and Williams, C., Using the special sensor microwave imager to monitor land surface temperature, wetness, and snow cover. *J. Appl. Meteorol.*, 1998, **37**, 888–911.
11. Badhwar, G. D., Crop emergence date determination from spectral data. *Photogramm. Eng. Remote Sensing*, 1980, **46**, 369–377.
12. Dubey, R. P., Ajwani, N. and Navalgund, R. R., Relation of wheat yield with parameters derived from a spectral growth profile. *J. Indian Soc. Remote Sensing*, 1991, **19**, 45–58.

13. Potdar, M. B., Sorghum yield modeling based on crop growth parameters determined from visible and near-IR channel NOAA–AVHRR data. *Int. J. Remote Sensing*, 1993, **14**, 895–905.
14. Shabanov, N. V., Zhou, L., Knyazikhin, Y., Myneni, R. B. and Tucker, C. J., Analysis of inter-annual changes in Northern vegetation activity observed in AVHRR data from 1981 to 1994. *IEEE Trans. Geosci. Remote Sensing*, 2002, **40**, 115–130.
15. Myneni, R. B., Los, S. O. and Tucker, C. J., Satellite based identification of linked vegetation index and sea surface temperature anomaly areas from 1982–1990 for Africa, Australia and South America. *Geophys. Res. Lett.*, 1996, **23**, 729–732.
16. Myneni, R. B., Tucker, C. J., Asrar, G. and Keeling, C. D., Inter annual variations in satellite sensed vegetation index data from 1981 to 1991. *J. Geophys. Res.*, 1998, **103**, 6145–6160.
17. Tucker, C. J., Fung, I. Y., Keeling, C. D. and Gammon, R. H., Relationship between atmospheric CO_2 variations and satellite driven vegetation index. *Nature*, 1986, **319**, 195–199.
18. Pettorelli, N., Vik, J. O., Mysterud, A., Gailard, J. M., Tucker, C. J. and Stenseth, N. C., Using the sattelite-derived NDVI to assess ecological responses to environmental change. *Trends Ecol. Evol.*, 2005, **20**, 503–510.
19. Smith, P. M., Kalluri, S. N. V., Prince, S. D. and DeFries, R. S., The NOAA/NASA Pathfinder AVHRR 8 km land data set. *Photogramm. Eng. Remote Sensing*, 1997, **63**, 12–31.
20. Gordon, H. R., Brown, J. W. and Evans, R. H., Exact Rayleigh scattering calculations for use with the Nimbus-7 coastal zone color scanner. *Appl. Opt.*, 1988, **27**, 2111–2122.
21. Rao, C. R. and Chen, J., Post launch calibration of the visible and near-infrared channels of the Advanced Very High Resolution Radiometer on NOAA-14 spacecraft. *Int. J. Remote Sensing*, 1996, **17**, 2743–2847.
22. Singh, R. P. and Dadhwal, V. K., Comparison of space-based Microwave Polarization Difference Index (MPDI) and Normalized Difference Vegetation Index (NDVI) for crop growth monitoring. *Indian J. Radio Space Phys.*, 2003, **32**, 193–197.
23. Basist, A., Garrett, D., Grody, N. C., Ferraro, R. R. and Mitchell, K., A comparison between snow cover products derived from visible and microwave satellite observations. *J. Appl. Meteorol.*, 1996, **35**, 163–177.
24. Wang, R. and Schmugge, T. J., An empirical model for the complex dielectric permittivity of soil as a function of water content. *IEEE Trans. Geosci. Remote Sensing*, 1980, **18**, 288–295.
25. Singh, R. P., Oza, S. R., Chaudhari, K. N. and Dadhwal, V. K., Spatial and temporal patterns of surface soil moisture over India estimated using surface wetness index from microwave radiometer (SSM/I). *Int. J. Remote Sensing*, 2005, **26**, 1269–1276.
26. Lakshmi, V., Wood, E. F. and Choudhury, B. J., Evaluation of special sensor microwave/imager data for regional soil moisture estimation over the red river basin. *J. Appl. Meteorol.*, 1997, **36**, 1309–1328.
27. Owe, M., Jeu, R. D. and Walker, J., A methodology for surface soil moisture and vegetation optical depth retrieval using the microwave polarization difference index. *IEEE Trans. Geosci. Remote Sensing*, 2001, **39**, 1643–1653.

ACKNOWLEDGEMENTS. We thank Dr R. R. Navalgund, Director, SAC, J. S. Parihar, Group Director, Agricultural Resources Group and Dr S. Panigrahy, Head, Agro-ecology and Management Division. Ahmedabad for encouragement and guidance. We are grateful to Dr V. K. Dadhwal, Indian Institute of Remote Sensing, Dehradun for guidance. We also thank the National Climatic Data Centre (NOAA/NESDIS) and Goddard Space Flight Center, Distributed Active Archive Centre for providing SSM/I wetness and NOAA–AVHRR data respectively.

Received 29 May 2006; accepted 5 August 2006

IgG4-reactive low molecular weight antigens from *Setaria digitata* adult parasites have immunodiagnostic potential in lymphatic filariasis

B. P. Mohanty[1,*], S. K. Dalai[2] and S. K. Kar

Center for Biotechnology, Jawaharlal Nehru University, New Delhi 110 067, India
[1]Present address: Central Inland Fisheries Research Institute, Biochemistry and Biotechnology Lab, Fish Health and Environment Division, Barrackpore 700 120, India
[2]Present address: Division of Immunology, Department of Pathology, John Hopkins University School of Medicine, Baltimore MD 21205, USA

Development of sensitive as well as low-cost immunodiagnostics for detection of infected individuals would be an important step towards reaching the goal of lymphatic filariasis elimination by 2020. In an earlier study, using soluble antigens of adult *Setaria digitata*, we have shown that an antigen fraction in the molecular weight range 14 to 20 kDa can induce differential Th1/Th2 immune response in the PBMC of the endemic normal (EN) and asymptomatic microfilaraemic (ASM) individuals residing in bancroftian filariasis endemic areas. In the present study, using 2D immunoblot we are able to show that two antigens of 17 and 18 kDa molecular weight and pI of 5–5.5 are recognized by the IgG4 isotype antibodies, a marker for active parasite infection, present in the sera of ASM but not in that of EN individuals. Elevated antigen-specific IgG4 antibodies in the blood are the indicators of circulating parasite in infected individuals who do not have apparent clinical symptoms of filariasis. Thus, we suggest that these two antigens can be explored for the immunodiagnosis of lymphatic filariasis.

Keywords: IgG4 isotype immunoblot, immunodiagnosis, low molecular weight antigens, lymphatic filariasis, *Setaria digitata*.

LYMPHATIC FILARIASIS (LF) is recognized as one of the world's most disabling diseases[1]. The disease is caused in humans by infection with the filarial nematode *Wuchereria bancrofti*, *Brugia malayi* or *Brugia timori* and continues to be a major public health problem in many of the tropical countries. The World Health Organization[2] has declared lymphatic filariasis to be the second leading cause of permanent and long-term disability worldwide and has targetted to eliminate LF globally by 2020. The disease manifests itself in a broad clinical spectrum. Individuals living in a filaria endemic area can be categorized on the basis of their clinical symptoms and parasitological as well as immunological profile into three broad groups, namely endemic normals (EN), asymptomatic microfilaremic individuals

*For correspondence. (e-mail: bimalmohanty12@rediffmail.com)